Demonstration of the antiferroelectric aspect of the helical superstructures in Sm-C^*, Sm-C^*_α, and Sm-C^*_a liquid crystals

Jan P. F. Lagerwall*

Institute of Physical Chemistry, University of Stuttgart, Pfaffenwaldring 55, D-70569 Stuttgart, Germany
(Received 14 May 2004; revised manuscript received 25 August 2004; published 4 May 2005)

We show that the helical superstructure in chiral smectic-C-type liquid crystal phases can, if the pitch is short enough, give rise to the tristate switching characteristic of antiferroelectrics even if the local commensurate order is synpolar as in the ordinary Sm-C^* phase. Since the field-induced helix unwinding exhibits a distinct threshold, in contrast to mere helix distortion, two unwinding / rewinding peaks per half cycle of an applied triangular wave voltage can be seen in the current response. By considering this antiferroelectric aspect of the helical modulation we give a simple explanation of why the ultrashort-pitch Sm-C^*_α phase exhibits antiferroelectric switching although its dielectric spectroscopy response is qualitatively identical to that of the synpolar Sm-C^* phase. Using data from the compound MHPOCBC we show that the Sm-C^*_α dielectric response is well described by continuum theory. We also demonstrate that, if the pitch is very short as in MHPOCBC, helix unwinding / rewinding leave characteristic traces in the electrooptic response even in the commensurately antiferroelectric (antipolar) Sm-C^*_a phase, distinguishable from the switching beween the antipolar and synpolar states of this phase.

I. INTRODUCTION

Liquid crystal compounds exhibiting the chiral smectic-C phase (Sm-C^*), characterized by a layered structure in which the director **n** is tilted with respect to the layer normal **k**, are often referred to as ferroelectric liquid crystals (FLCs) because they exhibit a spontaneous polarization $\mathbf{P}_s$ directed along $\pm\mathbf{k}\times\mathbf{n}$ [1,2]. However, the tilting direction and thus also the direction of $\mathbf{P}_s$ spiral about **k** in a helical fashion, leading to a cancellation of the polarization on a mesoscopic scale (microns) and rendering the phase helically antiferroelectric [3] or, by a shorter name, helielectric [4,5]. This is a special case of the general class of incommensurate antiferroelectrics [6,7]. Only in the surface-stabilized geometry, where the helix is suppressed by enclosing the liquid crystal between closely spaced planar-aligning substrates, may the Sm-C^* phase be regarded as ferroelectric in the usual meaning, i.e., it can then exhibit a strongly nonlinear response to an electric field as well as two stable states in absence of field [3,8,9].

Several variations of the chiral smectic-C phase exist, all of which are helielectric in bulk but which differ radically in terms of their local commensurate polar order. To distinguish it from the other variants, the basic Sm-C^* phase is often called *synclinic* and *synpolar*, referring to the lack of commensurate modulation (disregarding the slow helical precession, adjacent layers have the same directions of **n** and $\mathbf{P}_s$). The commensurately antiferroelectric Sm-C^*_a phase exhibits *anticlinic* order (alternating tilt direction in adjacent layers) and is thus *antipolar*. The phases Sm-C^*_α, Sm-C^*_β, and Sm-C^*_γ, finally, are often referred to as the chiral smectic-C "subphases." In the discussion of their polar nature the antiferroelectric aspect of the helical superstructures has been largely neglected. Although antiferroelectric switching has been observed in an ultrashort-pitch Sm-C^* material [10,11], such electro-optic response (three optically different states separated by peaks in the current response) is often taken as a sign of antipolar local order. This has had particularly adverse consequences for the understanding of the Sm-C^*_α phase, for which a complex picture has appeared which at best is compatible with selected experimental data.

In this paper we first present a Sm-C^* mixture with a helix pitch short enough to demonstrate the antiferroelectric aspect of the helical superstructure. The synpolar nature of the phase is verified by means of dielectric spectroscopy, but both the optic and the current response have the typical characteristics of antiferroelectric switching in thick samples. We then discuss what the prerequisites are for observing this type of helical-antiferroelectric switching and, by means of simple numerical modelling, we show that the response of a short-pitch Sm-C^* phase can look basically identical to that of Sm-C^*_a. As an experimental demonstration of this result, we present data from the Sm-C^*_α phase, which can be regarded as a low-tilt, ultrashort-pitch version of Sm-C^*, and in the same context we show that even in Sm-C^*_a the helielectric response can be observed—and distinguished from the switching of the local commensurate order—if the pitch is short enough. Although this response has been reported once before [12], it was never correctly explained. We finally discuss earlier reports of a complex polar nature of Sm-C^*_α in the light of the results.

II. EXPERIMENT

The short-pitch Sm-C^* liquid crystal used was a mixture (mixture 1) prepared from (S)-TFMHPOBC and ($1R,2R,3R,5S$)-IPC-16 [Fig. 1(a)] in molar ratio 72:28. During all experiments on this mixture the sample texture

---

*Electronic address: jan.lagerwall@ipc.uni-stuttgart.de

(S)-TMFHPOBC. P_S = +96 nCcm^{-2}
Cr. 87 Sm-C_a^* 114.5 Sm-A^* 123 Iso. / °C

(1R, 2R, 3R, 5S)-IPC-16. P_S = +50 nCcm^{-2}
Cr. 100 Sm-C^* 140.5 Sm-A^* 168 Iso. / °C

(R)-MHPOCBC. P_S = +61 nCcm^{-2}
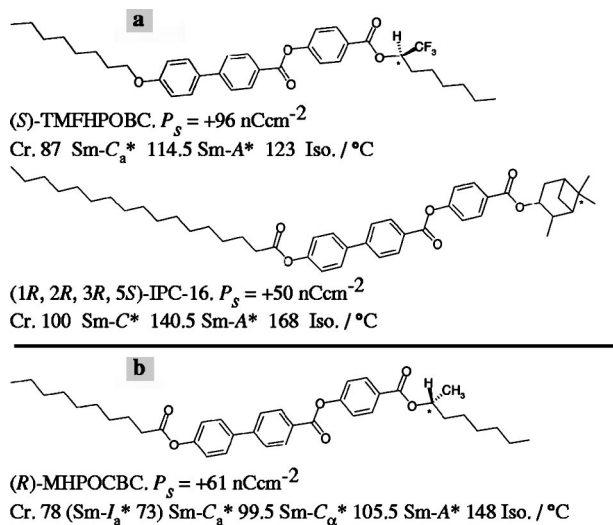Cr. 78 (Sm-I_a^* 73) Sm-C_a^* 99.5 Sm-C_α^* 105.5 Sm-A^* 148 Iso. / °C

FIG. 1. (a) The two chiral smectic liquid crystals which, blended together in 72:28 molar ratio, give the short-pitch Sm-C^* mixture 1. (b) (R)-MHPOCBC. Saturation values of spontaneous polarization P_s and phase sequences are listed for each molecule.

was monitored in order to verify that no demixing of the two components occurred. For investigations of the Sm-C_a^* and Sm-C_α^* phases (R)-MHPOCBC [Fig. 1(b)] was used. The materials were filled into cells with patterned transparent indium tin oxide (ITO) electrodes coated with antiparallelly buffed polyimide for planar alignment. For studies in homeotropic alignment simple glass slide samples were prepared. The selective reflection wavelength of these samples was measured with a multichannel optical analyzer (Lamda LS-2000) fitted to the microscope.

Dielectric spectroscopy measurements were carried out with an HP 4192A impedance analyzer and a Julabo HP-4 temperature controller. During these experiments the sample texture was automatically monitored with a digital camera mounted on the microscope and connected to the computer running the measurement software (DiScO, FLC Electronics), making the identification of phases and phase transitions more reliable. For electrooptic and current response measurements the samples were kept in an Instec mK2 hotstage mounted on an Olympus BH-2 polarizing microscope to which a photodiode (FLC Electronics) was fitted. The current was measured through a resistor connected in series with the sample. Current, optical response, and applied voltage were visualized with a Tektronix TDS420 oscilloscope.

III. RESULTS AND DISCUSSION

A. Tristate antiferroelectric switching in short-pitch helical Sm-C^*

The imaginary component of the complex dielectric permittivity $\epsilon' + i\epsilon''$ of mixture 1 is shown as a function of temperature and frequency in Fig. 2(a). Below the spectrum the results from fitting the imaginary single-mode Cole-Cole equation
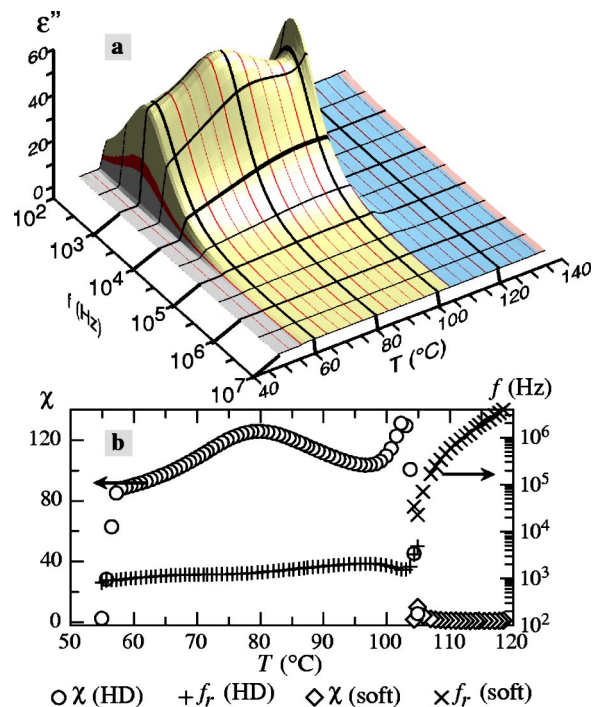

FIG. 2. (Color online) (a) The imaginary component of the dielectric permittivity of mixture 1 (23.5 μm sample) as a function of frequency and temperature, measured on cooling from the isotropic liquid (on-line version: pink spectrum surface color) to the crystalline phase (gray). The Sm-A^* phase (blue) is distinguished by the soft mode absorption, peaking at the transition to the Sm-C^* phase (yellow), the main absorption of which is the strong HD mode. (b) Results from fitting the Cole-Cole equation to the experimental data.

$$\epsilon'' = \frac{\chi (f/f_r)^{1-\alpha} \cos\left(\frac{\alpha\pi}{2}\right)}{1 + 2(f/f_r)^{1-\alpha}\sin\left(\frac{\alpha\pi}{2}\right) + (f/f_r)^{2(1-\alpha)}} \quad (1)$$

to the data are presented. Here χ is the (static) susceptibility of the mode [13], f is the frequency of the applied field, $f_r = 1/(2\pi\tau_r)$ where τ_r is the relaxation time of the mode, and α is the distribution parameter, taking values between 0 and 1 (α=0 corresponds to a Debye-type mode). The peak at 105 °C is due to the soft mode (field-induced fluctuations in θ, also called electroclinic effect) and indicates the low-temperature border of Sm-A^*. At lower temperatures, the absorption can be attributed to a helix distortion (HD) mode—often, somewhat inappropriately, referred to as Goldstone mode—clearly showing that here the phase is the synpolar helielectric Sm-C^*. This was also verified with miscibility tests in contact samples with reference liquid crystals exhibiting all of the different chiral smectic-C-type phases. For a HD mode, χ and f_r depend on P_s and the helical pitch p as [15,16],

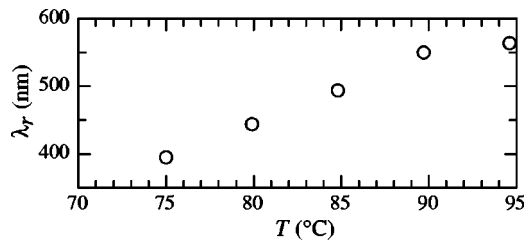$$\chi = \frac{1}{8\pi^2 K_\varphi \epsilon_0}\left(\frac{P_s p}{\theta}\right)^2, \quad (2)$$

FIG. 3. The wavelength of selective reflection λ_r of mixture 1 as a function of temperature. The helical pitch of the Sm-C^* **n**-$\mathbf{P}_s$ modulation can be obtained by dividing λ_r by the average refractive index.

$$f_r = \frac{2\pi K_\varphi}{\gamma_\varphi p^2}, \tag{3}$$

where K_φ and γ_φ are the elastic constant and viscosity, respectively, relevant for azimuthal fluctuations of **n**, and θ is the director tilt angle.

The pitch p was determined by measuring the wavelength of selective reflection λ_r of a homeotropically aligned sample. On decreasing the temperature λ_r decreased monotonically, cf. Fig. 3. Below 75 °C it could no longer be studied as it was then in the UV range, outside the transparency window of the microscope lenses. Based on the data in the visible range we can estimate λ_r between 55 and 60 °C to about 300 nm. We then obtain, using a typical average refractive index value of 1.5, a pitch of the helical **n**-$\mathbf{P}_s$ modulation around 200 nm in this temperature region, whereas it is close to half a micrometer just below the Sm-A^* phase.

The electro-optic response to an applied triangular wave voltage was investigated using planar-aligned samples of 4, 10, and 23.5 μm thickness. The Sm-C^* phase was helical under static field-free conditions in all three samples, as verified by texture observation. Nevertheless, the 4 μm sample exhibited mainly ferroelectriclike switching at all Sm-C^* temperatures, indicating that this sample switched more or less directly between the two field-induced synclinic states. At low temperatures, where p reaches its lowest value, a distinct shoulder could, however, be distinguished at the end of the polarization peak [Fig. 4(a)], suggesting a certain degree of relaxation to an intermediate state even under dynamic conditions. This tendency grew stronger on increasing the cell gap, to the extent that the 10 and 23.5 μm samples both exhibited antiferroelectriclike switching at low temperatures of the Sm-C^* phase: the current response [Figs. 4(b) and 4(c)] had two quite well separated peaks per half-cycle, most distinct in the thicker sample [17]. Obviously, the short-pitch Sm-C^* helix of mixture 1 could in these thicker cells rewind once per half-cycle of the switching process, allowing the demonstration of the antiferroelectric aspect of the helical superstructure. However, whereas the second, smaller, peak can be attributed fully to helix unwinding, the first, larger, peak is only in part due to rewinding. The difference in peak area shows that a large part of the sample switched directly between the two end states without intermediate helix formation, also at these cell gaps. Such switching contributes only to the first peak.
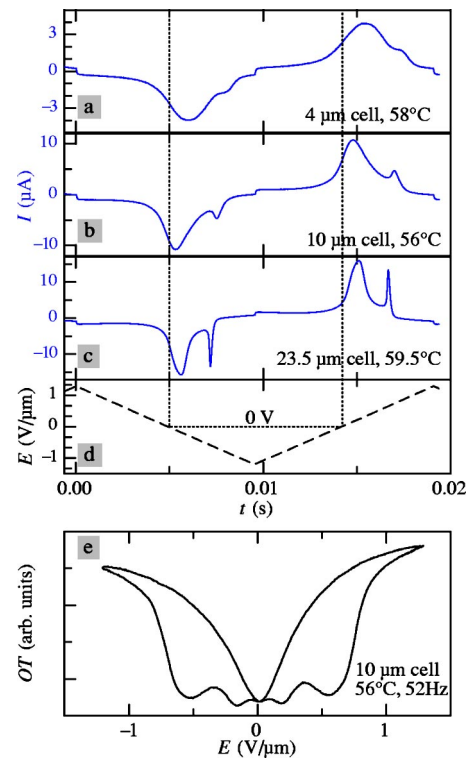

FIG. 4. Current (a, b, c) and optical transmission (e) response of mixture 1 to a 52 Hz triangular wave voltage (d) at temperatures where the Sm-C^* pitch is close to its lowest value. The twin peaks per half cycle in the current response, characteristic of antiferroelectric switching, are easy to see with 10 and 23.5 μm samples, but at 4 μm cell gap they cannot be clearly resolved. The butterflylike optical transmission response of the 10 μm sample shows that three basic states are passed in the switching process: the two fully switched uniform synclinic states (bright) and the helical low-voltage state (dark).

Figure 4(e) shows the optical transmission response of the 10 μm sample, aligned with **k** parallel to the polarizer, measured with light of wavelength $\lambda = 589$ nm. It has a "butterflylike" shape, showing that there are three basic "states" during the switching process. The two fully switched states exhibited roughly the same transmission (the slight difference is due to imperfect alignment). The intermediate "state" (between ~ 0 and $\sim \pm 6$ V applied voltage) was where parts of the sample formed the helical geometry, lowering the overall transmission since the effective optic slow axis in this geometry is along **k**, thus along the polarizer. The electro-optic response of this short-pitch Sm-C^* phase demonstrates that switching behavior as in Figs. 4(c) and 4(e) cannot be taken as an unambiguous sign of commensurate antiferroelectricity, nor does a response like in Figs. 4(a) and 4(b) indicate ferrielectricity, an interpretation which has not been uncommon so far.

In a solid-state commensurate antiferroelectric the switching threshold corresponds to the energy barrier between the anti- and synpolar states. There are no intermediate states. Once the threshold is passed one of the two sublattices reverses its polarization direction, giving a contribution to the current of two times $P_s/2$. The closest liquid crystal approxi-

mation to this case is the Sm-C_a^* phase. The characteristic current response to a triangular wave voltage of this phase exhibits two polarization reversal current peaks per half cycle, each with an area roughly corresponding to P_s. However, surface pinning effects often influence the symmetry and the areas of the peaks. Moreover, the helical superstructure can have an impact on the response also in Sm-C_a^*, as will be shown below.

In a helical Sm-C^* sample, on the other hand, the polarization cancellation is due solely to the incommensurate helical superstructure, and this can be heavily distorted already by a weak electric field, thereby giving rise to the strong small-signal dielectric response (the response is linear). There is no threshold for the initial distortion of the helix, only for its complete unwinding [18]. The peaks in the helielectric Sm-C^* current response thus correspond to the expulsion of an already distorted helical structure and its reforming, hence, the areas of these peaks should be somewhat smaller than the P_s area. In order to get a feeling for what area we can expect we will do a short numerical analysis of the situation.

The distorted helical structure as well as the unwinding step has been studied extensively, with and without taking the influence of the sample boundaries into account [2,4,19–24] but the helielectric switching peak areas have never been calculated. In our case we are interested in the special case of materials with p so short that the liquid crystal-surface interaction can be neglected in a first approximation. We can thus use one-dimensional expressions describing how the bulk liquid crystal responds to an applied electric field. Even in this case analytical solutions are not available but by numerically integrating, e.g., the expressions of Fünfschilling and Schadt [23],

$$\frac{1}{L}\frac{\partial z}{\partial \varphi} = \left(\sqrt{1 - k^2 \sin \varphi} \int_0^{2\pi} \frac{d\varphi}{\sqrt{1 - k^2 \sin \varphi}} \right)^{-1}, \quad (4)$$

$$\frac{E}{E_c} = 32k^2 \left(\int_0^{2\pi} \sqrt{1 - k^2 \sin \varphi}\, d\varphi \right)^{-2}, \quad (5)$$

we can get a good picture of what the distorted structure looks like just before unwinding the helix. In these expressions L is the field-dependent periodicity along the layer normal ($L > p$ for nonzero fields), z is the position along the layer normal, φ is the azimuthal angle of **n**, defined such that $\varphi = 90°$ for the fully unwound structure where $\mathbf{P}_s$ points along the applied field, and k is a dimensionless parameter between 0 and 1 which describes the strength of the applied field in terms of the unwinding field E_c. This threshold level (corresponding to $k = 1$) is given by [23],

$$E_c = \frac{\pi^4 K_\varphi}{4p^2 P_s}. \quad (6)$$

In Fig. 5 we show the $\sin \varphi(z/L)$ function resulting from the numerical integration of (4) for some field strengths varying from $k = 0$ to $k = 0.999$. The $\sin \varphi$ function gives the contribution of each smectic layer to the effective macroscopic polarization $P_m = \langle \sin \varphi \rangle P_s$. For fields close to the unwinding
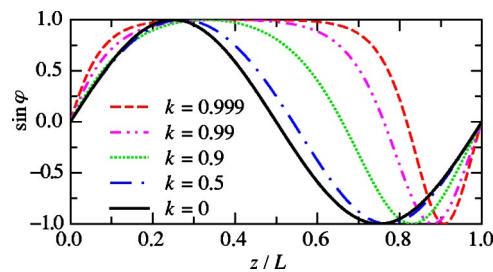

FIG. 5. The value of $\sin \varphi$ as a function of the distance along the layer normal (z) divided by the periodicity of the sample in this direction (L), in the absence of field ($k = 0$) and for four different levels below the unwinding threshold ($k = 1$). The function $\sin \varphi(z/L)$ expresses the contribution of each layer polarization to the macroscopically measured polarization.

threshold the **n**-$\mathbf{P}_s$ couples are almost uniformly aligned within certain regions, as shown by $\sin \varphi$ lying almost constantly at 1, but between two such regions the structure twists rapidly. These tightly twisted walls are spatial solitons [4,22]. The helical-antiferroelectric threshold now corresponds to expelling the solitons from the structure, i.e., unwinding, not just distorting, the helix. If we start from the relaxed helical structure and apply an increasingly strong voltage, the current response will exhibit a peak when the unwinding threshold is passed, reflecting the polarization contained in the solitons. Starting from relations (4) and (5) it is easy to obtain the average value $\langle \sin \varphi \rangle$ at a selected field strength. At $k_1 = 0.999$, which according to (5) is equivalent to $E = 0.995E_c$, the average $\langle \sin \varphi \rangle_{k_1} \approx 0.59$. Hence, the area of the helix unwinding current peak can be expected to reach values corresponding to about $2(1 - \langle \sin \varphi \rangle_{k_1})P_s \approx 0.8P_s$, i.e., quite close to the situation in commensurate antiferroelectrics, as described above.

The prerequisite for the unwinding peak reaching such an area in a switching experiment is that the helical structure reforms throughout the sample when the driving voltage passes zero and changes sign. In most Sm-C^* samples this is not the case. Due to the action of the surfaces to stabilize the nonhelical structure, the helix generally does not reform at all during the switching process and, consequently, only one polarization peak, corresponding to direct switching between the synpolar end states, is observed.

B. The helielectric response of Sm-C_α^*

In order to approach the maximum helix unwinding peak area we obviously need p to be much smaller still than in mixture 1. We could then expect the first peak (rewinding) and the second (unwinding) to be quite similar in area. Moreover, the peaks may be better separated in time since the helix rewinding should be more likely to occur before the driving voltage reaches zero. Hence, the current response of such a helielectric sample can look very similar to the typical Sm-C_a^* response. A phase which has such a short helix pitch is the Sm-C_α^* phase, appearing in a small temperature range directly below Sm-A^* in many chiral smectics. Although still not fully understood, recent experimental work, in particular resonant x-ray scattering and ellipsometry experiments, have

made it relatively clear that the only type of director modulation in Sm-C_α^* is a very rapid smooth variation of the tilt direction, incommensurate with the smectic layer spacing, giving the structure a very short helical period, typically between 5 and 50 smectic layers [25–35]. Thus, the Sm-C_α^* phase is structurally an extreme version of short-pitch Sm-C^*.

However, its electro-optic switching behavior was early on reported to change from antiferroelectric to ferrielectric on cooling through the temperature range of the phase [12,36–38] and based on these reports (which will be discussed in more detail in Sec. III D) the local polar structure of Sm-C_α^* was conjectured to change radically within the phase. Although this idea is contradicted by the dielectric spectroscopy response of the phase, exhibiting a fairly weak but nevertheless clearly polar mode [39], and though it is difficult to understand it within the view of Sm-C_α^* as a phase with only a short-pitch helical modulation, this conjecture has been the starting point for many experimental investigations as well as for the development of quite complex theoretical models [12,34,38,40–47]. Applying the results of the preceding section to Sm-C_α^* we can now give a much simpler explanation to the antiferroelectric switching behavior and we can easily reconcile this with its polar dielectric response, without any need for modification of the generally accepted view of the phase.

An excellent compound for investigating the switching in SmC$_\alpha^*$, as well as in the Sm-C_a^* phase, is MHPOCBC. This compound exhibits a relatively broad Sm-C_α^* phase (6 K) and a direct Sm-C_α^*-Sm-C_a^* transition. The dielectric absorption spectra, as obtained on heating and on cooling a thick sample, together with Cole-Cole fitting results are presented in Fig. 6. The Sm-C_α^* phase (on-line version: purple in a and b) is easily distinguished from the antipolar, and hence, essentially absorption-free, Sm-C_a^* phase (green) by its absorption which we can attribute to distortion of the helical structure (HD mode).

We note the striking qualitative similarity of the Sm-C_α^* cooling spectrum with the Sm-C^* spectrum in Fig. 2, reflecting the fact that the phases have the same basic structure. Quantitatively, the Sm-C_α^* HD mode has more than an order of magnitude smaller χ and two orders of magnitude higher f_r, differences we can attribute to the much smaller pitch, c.f. Eqs. (2) and (3). The elastic constant K_φ in these equations as well as in Eq. (6) is the smectic elastic constant B_3 counteracting a change in the twist of the **c** director (the projection of **n** on the smectic layer plane). Expressed in the Oseen-Frank constants it can be written as (c.f. p. 293 in Ref. [9]),

$$K_\varphi \equiv B_3 = K_{22}\sin^4\theta + K_{33}\sin^2\theta\cos^2\theta. \qquad (7)$$

In general it thus contains contributions from both twist and bend. However, in the case of Sm-C_α^*, where the tilt angle θ is of the order of 5 deg, we can use this relation in the limit of small θ, where it reduces to

$$K_\varphi \approx K_{33}\theta^2. \qquad (8)$$

In the small-angle limit the elastic constant K_φ thus represents pure bend, and it has the same θ dependence as the viscosity which scales as $\gamma_\varphi = \gamma\sin^2\theta$ (c.f. p. 178 in Ref.
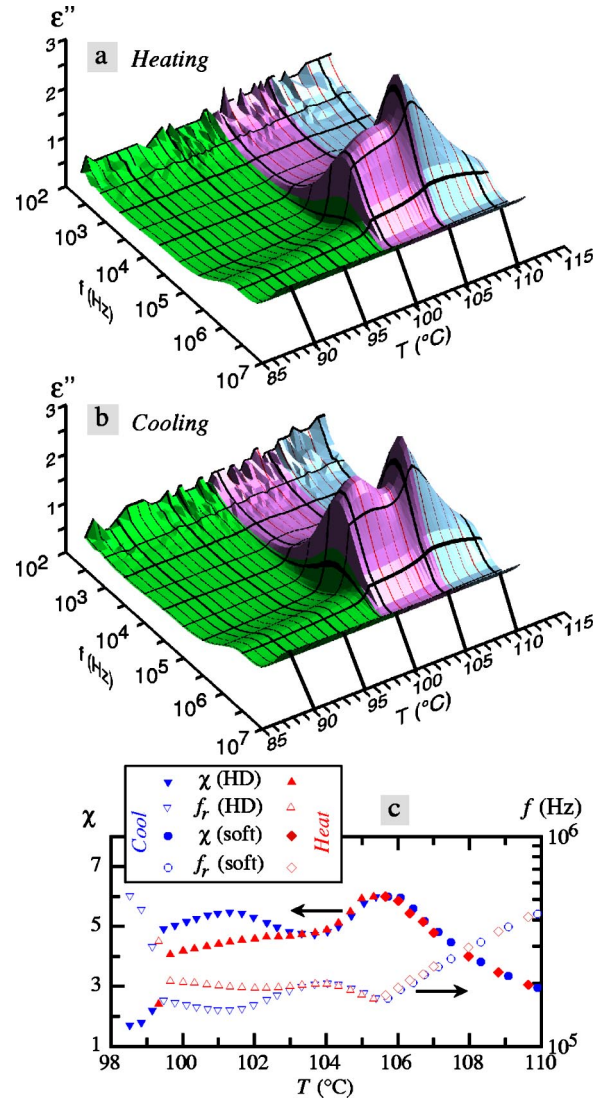

FIG. 6. (Color online) The imaginary component of the dielectric permittivity of MHPOCBC (23.5 μm sample) as a function of frequency and temperature, measured on heating (a) and cooling (b) between the absorptionless Sm-C_a^* phase (on-line version: green) and Sm-A^* (blue), dominated by the soft mode. Results from fitting the Cole-Cole equation to the data are shown in (c). The absorption around 200 kHz in Sm-C_α^* (purple) results from distortion of the short-pitch helix and shows that this phase does not exhibit antipolar local order like the Sm-C_a^* phase.

[9]). Their ratio, which is the relevant quantity in Eq. (3), can thus be expected to be relatively similar in Sm-C^* and Sm-C_α^*. Inserting standard Sm-C^* values for K_φ and γ_φ into (3) we can then use the dielectric spectroscopy results to get a rough estimate of the Sm-C_α^* helix pitch. With a typical bend constant of $K_{33} = 10$ pN and with $\gamma \approx 1$ Ns/m^2 we find a p value of about 18 nm, corresponding to about six layers. A very similar value results by entering measured values for χ, P_s and θ in (2). Such a short pitch is expected for the Sm-C_α^* phase, hence, its dielectric absorption is both qualitatively and quantitatively in agreement with the response expected from field-induced helix distortion.

The Sm-C_α^* HD mode reaches a slightly larger susceptibility and a lower value of f_r on cooling than on heating, suggesting that the transition from the antipolar Sm-C_a^* phase has an influence on the Sm-C_α^* pitch in the heating experiment. Similar memory effects between other chiral smectic-C-type phases have been demonstrated using dielectric spectroscopy with simultaneous texture monitoring [48]. By investigating flat droplets of compounds exhibiting the Sm-C_α^* phase with a sophisticated optical technique, Laux *et al.* showed that the periodicity of the Sm-C_α^* helical structure depends sensitively on the history of the sample: the "natural" structure develops only when the phase is formed on cooling from Sm-A^*, whereas the development on heating depends on what chiral smectic-C-type phase precedes Sm-C_α^* [42]. Their general observation was that p on heating was very small and relatively constant, whereas it exhibited a stronger temperature dependence with a maximum in the low-temperature half of the phase if the sample was cooled from Sm-A^*. According to Eqs. (2) and (3) such a $p(T)$ behavior would result in just the type of response seen in Sm-C_α^* in Fig. 6.

The success of continuum elasticity theory for modeling the Sm-C_α^* response may seem surprising, considering that a helical period as short as six layers corresponds to an azimuthal angle difference $\Delta\varphi$ of 60 deg from layer to layer. At first sight this would suggest huge discontinuities in the director field. However, $\Delta\varphi$ by itself gives a misleading picture of the real structure. If the very small tilt in Sm-C_α^* is taken into account one finds that the actual reorientation of **n** from one layer to the next is only about 5 deg [49]. This is a quite normal value in helielectric structures, to which the continuum description is appropriate. Furthermore, one should remember that smectics have a rather low degree of translational order; the density modulation along **k** is often more or less sinusoidal. Although the structures of the various chiral-smectic-C-type phases are generally illustrated with perfectly sharp layer boundaries, suggesting that discrete treatments of these phases would be the most adequate, the real situation is thus much more continuous, with a substantial number of molecules at any instant being right between two layers.

The electro-optic response of MHPOCBC was continuously monitored as the sample was heated at a constant slow rate (0.2 K/min) from Sm-C_a^* to Sm-A^*, via the Sm-C_α^* phase. The resulting current response data, obtained with a 10.5 Hz, ± 6.8 V/μm triangle wave switching field applied to a 23.5 μm thick sample, is plotted in Fig. 7. Apart from a small temperature range in the vicinity of the Sm-C_a^*-Sm-C_α^* transition, where phase coexistence affected the response, the Sm-C_α^* current followed a clean antiferroelectric response curve with two well separated peaks appearing on opposite sides of the 0 V level of the applied field. The threshold for helix unwinding decreased from about 3 V/μm to less than 1 V/μm just before the transition to Sm-A^*. Since P_s rapidly decreased in the same process, Eq. (6) shows that this change in threshold must be generated by a strong decrease in K_φ and/or an increase in p. Most likely, the origin lies mainly in the former parameter which, according to (8) depends strongly on θ, rapidly decreasing on heating towards the untilted Sm-A^* phase.
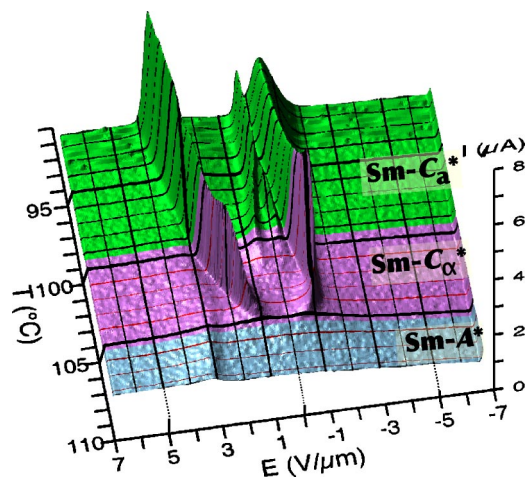

FIG. 7. (Color online) The current response of (R)-MHPOCBC to the increasing *half*-period (time goes from right to left on the E axis) of a 10.5 Hz triangular wave driving field as a function of temperature, on heating at a constant rate of 0.2 K/min. The sample was 23.5 μm thick, enough for achieving bulk response.

The helix rewinding peak voltage was less dependent on temperature, but instead its shape changed more than that of the unwinding peak. About 3 K below the Sm-C_α^*–Sm-A^* transition the peak height was the maximum observed in the experiment, illustrating that the rewinding here was actually a much faster process than unwinding. Towards lower temperatures the peak broadened and decreased somewhat in height, indicating that helix reformation was more hindered, hence, more extended in time, as P_s and θ increased. The integrated areas of the unwinding and rewinding peaks were similar throughout the phase amounting to ~0.7–0.9 times P_s [50], in good agreement with the modeling in Sec. III A.

C. The superposition of commensurate and incommensurate antiferroelectricity in Sm-C_a^*

The Sm-C_a^* phase in MHPOCBC exhibits not only two, but three to four peaks per half-period of the switching voltage. Following the discussion above, we can understand the additional small peaks at low voltage in terms of helix rewinding and unwinding preceding the antipolar-synpolar switching. The helical superstructure and the local antipolar order makes the Sm-C_a^* phase antiferroelectric on two scales, incommensurate antiferroelectricity superposed on commensurate, hence, two sets of antiferroelectric polarization peaks are possible.

To understand why also the Sm-C_a^* phase can give polarization peaks at helix unwinding and rewinding we must consider the intermediate switching state where the helix is unwound but the synclinic/synpolar state is not yet reached. This state has been discussed in detail by Zhang *et al.*, Wen *et al.*, and Rudquist *et al.* [51–53], showing that it is characterized by a deviation from perfectly antipolar order resulting in a nonzero residual macroscopic polarization, here denoted $\mathbf{P}_r$. (Note that $\mathbf{P}_r$ should not be confused with the bilayer residual polarization of the helical state, which reverses at every layer boundary and thus gives no macroscopic contri-
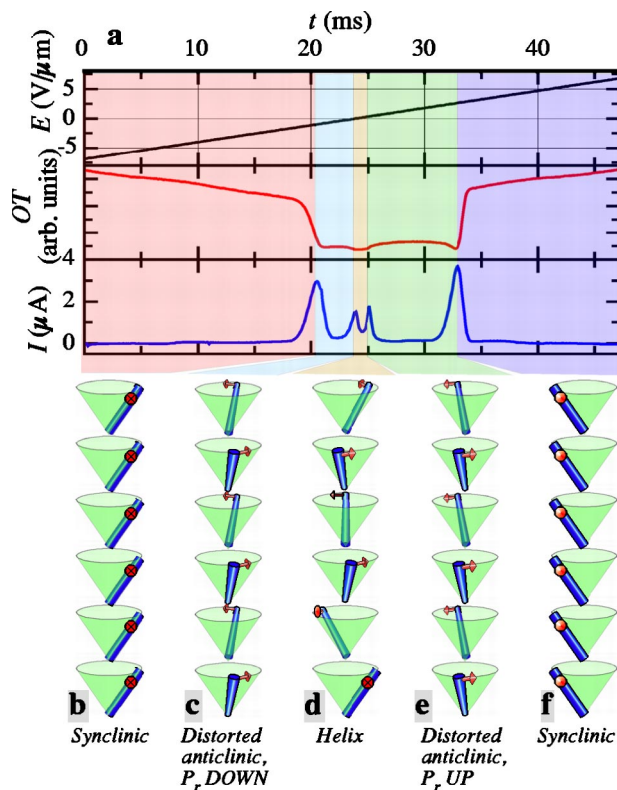
FIG. 8. (Color online) Current I (lower curve) and optical transmission OT (middle curve) at $\lambda = 633$ nm through the 10 μm MH-POCBC sample between crossed polarizers (parallel and perpendicular to the layer normal), during an increasing half period of the applied 10.5 Hz triangular wave field (top curve), at 99 °C. At the bottom schematic cartoons illustrate the five different states gone through during the switching process.

bution.) This intermediate macroscopically polar state is equivalent to one of the field-induced Sm-C_a^* states which resulted from a theoretical treatment by Boulbitch and Tolédano [54]. Following exactly the same reasoning as developed in Sec. III A for helical Sm-C^*, we realize that also the Sm-C_a^* helix unwinding can give rise to a current peak, albeit of smaller magnitude since it is only $P_r \ll P_s$ that is released as the solitons are expelled. In contrast to $\mathbf{P}_s$, $\mathbf{P}_r$ is directed into the tilt plane (the generalized tilt plane of Ref. [53], to be precise), hence, the nonhelical but not synclinic state is characterized by a vertical tilt plane and an effective optic slow axis which is tilted away slightly from the layer normal, cf. Figs. 8(c) and 8(e), and Ref. [53]. This leads to a small increase in transmission between crossed polarizers, aligned parallel and perpendicular to the smectic layer normal.

In Fig. 8 one half-cycle of the Sm-C_a^* current and optical response of a 10 μm sample at 99 °C is shown, together with illustrations of the different states as the sample is driven from one fully switched, synclinic, and synpolar, state to the other. The first large current peak occurs at relaxation to the distorted antipolar state without helix. Somewhat later the helix rewinds, giving the first small peak corresponding to $\mathbf{P}_r$, but it is again unwound just after the driving voltage has changed sign, producing the second small $\mathbf{P}_r$ peak. As the

voltage is further increased the distortion of the antipolar state grows, producing a gradual change in the optical response (which can be related to changes both in slow axis direction and in birefringence), until the threshold for switching to the synclinic state is reached at about 3 V. The ratio of the areas of the small and large peaks is about $1:5$ (exact measurements are difficult to do because of peak overlap) and $\mathbf{P}_r$ is thus about $\mathbf{P}_s/6$. A simple geometrical calculation shows that this relation corresponds to a deviation from the fully antipolar state of about 10° in the nonhelical but not synclinic state.

From Fig. 7 it is clear that the two helix rewinding-unwinding peaks are well separated only at high temperatures within Sm-C_a^*. At lower temperatures the relaxation is obviously too slow, such that helix rewinding cannot occur before the applied voltage changes sign. The structure is then switched directly from state (c) to state (e) in Fig. 8, giving only one peak with an area corresponding to $2P_r$ between the two major peaks in the current response. The slowing-down on cooling applies also to the relaxation of the commensurate structure from syn- to distorted antipolar, the peak of which broadens considerably on cooling until its tail extends past the time of driving voltage sign change, at about 95 °C.

One may ask why the helix-related peaks are generally not observed in switching experiments on the Sm-C_a^* phase. The reason is the same as why antiferroelectriclike current response is normally not seen from Sm-C^* samples: the helix must have an exceptionally short pitch to rewind during switching. The pitch of MHPOCBC is short not only in the Sm-C_α^* phase but also the Sm-C_a^* phase has an exceptionally small value of p. It is much smaller than optical wavelengths, rendering the homeotropic texture black without any schlieren. Based on null transmission ellipsometry data, Cady *et al.* estimated it to about 50 smectic layers [33].

D. Comparison with previous views of Sm-C_α^*

If the Sm-C_α^* phase is simply short-pitch helielectric one must ask why so many reports of ferrielectriclike behavior at low temperatures of this phase exist and why it was believed that Sm-C_α^* is not a single phase but has low and high-temperature ranges exhibiting different local polar properties. The observations which have been taken as evidence for ferrielectricity are mainly mixed current response [12,38,47], complex field-dependence of the apparent tilt angle [12,37,44,55], and a characteristic field dependence of the optical index ellipsoid detected by conoscopy [37,46]. As for the mixed current response, it is probably mainly a result of phase coexistence or difficulties in accurately determining the phase in which an experiment is performed. It has been clearly demonstrated that surfaces can have a considerable impact on the phase sequence of compounds exhibiting multiple chiral smectic-C-type phases, in such a way that synpolar Sm-C^* is favored over the other variants [48,56–58]. To rule out phase coexistence effects measurements must thus be performed on relatively thick cells.

Moreover, the by far most commonly studied compound is MHPOBC, a compound where the Sm-C_α^* phase range is small (~ 1 K), usually with Sm-C^* following on cooling, and

which is known to have a phase sequence very sensitive to sample purity [59,60]. The reports referring to the low-temperature region of Sm-C_α^* in MHPOBC are thus very likely to be based on measurements where Sm-C_α^* and Sm-C^* coexisted. MHPOCBC is a much better compound for studies of Sm-C_α^* since it lacks the Sm-C^* phase, and if one scrutinizes the reports on this compound no clear indications of ferrielectric behavior can be found. In Ref. [12] current response curves from MHPOCBC containing the smaller twin peaks at low voltage—explained above as a result of Sm-C_a^* helix unwinding and rewinding—are shown and taken as a sign of ferrielectricity of Sm-C_α^*. It is, however, clear from the data in Fig. 7 that the low-voltage peaks are a characteristic of the Sm-C_a^* phase, not of Sm-C_α^*. Indeed, the four-peak MHPOCBC response curves in Ref. [12] are obtained at temperatures 96–97 °C, i.e., in Sm-C_a^*.

The observation that θ jumps abruptly above a threshold field at low temperatures while it varies smoothly at high temperatures within the Sm-C_α^* phase [12,37,46,55] can be understood by considering the fact that the main contribution to the apparent tilt comes from the threshold-free electroclinic effect at high temperatures, whereas it is the helix deformation and unwinding—the latter process giving the threshold—that dominate at low temperatures. Reports of additional complex θ behavior at the very low-temperature boundary of the phase [46,55] are again most likely a result of phase coexistence, as evidenced by the fact that such behavior was only observed at one particular temperature at the phase transition.

The peculiar conoscopy behavior, finally, amounts to an isogyre splitting along the electric field for intermediate field strength, whereas it is perpendicular to the field at strong fields. This behavior has been explained as a result of the electroclinic effect imposing a substantial and complex modulation of the tilt angle at field strengths below the threshold for unwinding the ultrashort-pitch Sm-C_α^* helix [56]. Because the structure is helical, in contrast to Sm-A^*, the electroclinic effect leads to tilt angle increase in some layers, but to a decrease in others, an effect producing the unusual conoscopy pictures.

Because of the small temperature range of Sm-C_α^* and its close vicinity to the untilted Sm-A^* phase, θ and P_s—the order parameters of the phase—vary strongly with temperature, which may lead to further complications. These parameters have a strong impact on the helix unwinding and rewinding mechanisms as well as on surface pinning effects. If the frequency or amplitude of the driving field is high, the characteristic antiferroelectric response can be lost at low temperatures and replaced by a mixed response (ferrielectric-clike), ultimately a ferroelectric response.

Recently a report on field and temperature dependent mesurements of birefringence, Δn, on homeotropically aligned MHPOCBC was presented as evidence for a multiphase nature of Sm-C_α^* [43]. The temperature range which in that paper is referred to as the low-temperature Sm-C_α^* part coincides well with the range over which the HD mode was particularly strong in Fig. 6(b). The variation of the HD mode characteristics seen on cooling is the only observation in the present study that could be taken as a sign of substantial temperature dependence of the Sm-C_α^* phase behavior.

However, the absence of such variation on heating and the fact that the same type of temperature dependence of the Sm-C^* HD mode was seen in the cooling experiment on mixture 1 in Fig. 2 show that this variation is not a sign of multiphase behavior. Rather, it should be attributed to the fact that the HD mode can be weaker than the soft mode if p and P_s are small, as is the case close to Sm-A^* in Figs. 2 and 6, whereas it dominates the spectrum at lower temperatures where P_s is larger. The same subtle balance between electroclinic and HD response, together with the temperature dependence of θ throughout the Sm-C_α^* phase, can explain the observations in Ref. [43]. The birefringence of a homeotropically aligned sample depends sensitively on the tilt, through $\Delta n \sim \theta^2$, as well as on the type of helical structure that is present, hence, a complex behavior of Δn is to be expected as temperature and electric field strength are varied.

IV. CONCLUSIONS

In this work we have demonstrated the impact of the helical superstructure on the switching behavior of the Sm-C^*, Sm-C_α^*, and Sm-C_a^* liquid crystal phases. If the pitch is short the incommensurate antiferroelectric aspect of the helix can produce a double hysteresis in the electro-optic response and twin peaks in the current response, i.e., the characteristics of antiferroelectric switching, even in Sm-C^*. Such switching behavior alone is thus no proof of commensurate local antipolar order, and a mixed switching response is no proof of ferrielectric order. Based on these observations the electro-optic and dielectric behavior of the Sm-C_α^* phase can be explained qualitatively and quantitatively simply as a result of helix distortion at low field strength, and unwinding / rewinding at high field strength. The conjecture that this phase would be antiferroelectric at high temperatures but ferrielectric at low temperatures can thus be replaced by the insight that the behavior of the phase reflects its helielectric structure, ultrashort pitch, and very small director tilt. The terms ferro-, ferri-, and antiferroelectric, developed in the state of polar solid crystals and applying to their macroscopic properties (in conformity with one or several possible meso- or microscopic model structures), can obviously lead to some confusion when used for describing the local polar order of chiral smectics. A clearer picture can be conveyed by speaking of syn- and antipolar organization, or by clearly distinguishing between commensurate and incommensurate polarization modulation.

[1] R. B. Meyer, L. Liebert, L. Strzelecki, and P. Keller, J. Phys. (Paris), Lett. **36**, L69 (1975).

[2] R. B. Meyer, Mol. Cryst. Liq. Cryst. **40**, 747 (1977).

[3] N. A. Clark and S. T. Lagerwall, Appl. Phys. Lett. **36**, 899 (1980).

[4] P. E. Cladis and W. van Saarloos, in *Solitons in Liquid Crystals*, edited by L. Lam and J. Prost (Springer-Verlag, New York, 1992), pp. 110–150.

[5] H. R. Brand, P. E. Cladis, and P. L. Finn, Phys. Rev. A **31**, 361 (1985).

[6] G. A. Smolenskii, V. A. Bokov, V. A. Isupov, N. N. Krainik, R. E. Pasynkov, and A. I. Sokolov, *Ferroelectrics and Related Materials* (Gordon and Breach, New York, 1984).

[7] The terminology for polar liquid crystals has superficially been taken over from the much more established one for polar solids but it did not develop in a very systematic way as more complex polar liquid crystal structures were found. Solids in which $\mathbf{P}_s$ varies periodically in space, incommensurately with the crystal lattice, such that the macroscopic polarization averages to zero belong to the broad class of antiferroelectrics. Such incommensurate antiferroelectrics, of which helical Sm-C^* is an analog example, are discussed, e.g., by Smolenskii *et al.* (see Ref. [6]). The regular helical superstructure, being inherent to the phase, is not comparable to the irregular separation into domains on a macroscopic scale observed in ferroelectrics.

[8] M. E. Lines and A. M. Glass, *Principles and Applications of Ferroelectrics and Related Materials* (Clarendon Press, Oxford, 1977).

[9] S. T. Lagerwall, *Ferroelectric and Antiferroelectric Liquid Crystals* (Wiley-VCH, Weinheim, 1999).

[10] K. Itoh, Y. Takanishi, J. Yokoyama, K. Ishikawa, H. Takezoe, and A. Fukuda, Jpn. J. Appl. Phys., Part 2 **36**, L784 (1997).

[11] M. Zennyoji, J. Yokoyama, Y. Takanishi, K. Ishikawa, H. Takezoe, and K. Itoh, Jpn. J. Appl. Phys., Part 1 **37**, 6071 (1998).

[12] A. Fukuda, Y. Takanishi, T. Isozaki, K. Ishikawa, and H. Takezoe, J. Mater. Chem. **4**, 997 (1994).

[13] In their original paper (see Ref. [14]), the brothers Cole wrote the difference between the static and high-frequency dielectric permittivity, $\epsilon_0 - \epsilon_\infty$, instead of χ. Here we use the fact that $\chi = \epsilon_0 - \epsilon_\infty$ for a more compact notation.

[14] K. S. Cole and R. H. Cole, J. Chem. Phys. **9**, 341 (1941).

[15] A. Levstik, T. Carlsson, C. Filipic, I. Levstik, and B. Zeks, Phys. Rev. A **35**, 3527 (1987).

[16] T. Carlsson, B. Zeks, C. Filipic, and A. Levstik, Phys. Rev. A **42**, 877 (1990).

[17] In addition to the cell gap, the frequency f and amplitude A of the applied field influenced the response. At A just high enough for complete switching it became difficult to distinguish the two peaks at f above ~ 200 Hz in the 23.5 μm cell. Decreasing f to 1 Hz had no qualitative influence on the response; the first peak still occurred after the sign change of the driving voltage. In the 4 μm cell the shoulder could be clearly detected up to $f \sim 100$ Hz.

[18] A. Jakli, S. Markscheffel, and A. Saupe, J. Appl. Phys. **79**, 1891 (1996).

[19] B. I. Ostrovsky, S. Pikin, and V. G. Chigrinov, Sov. Phys. JETP **50**, 811 (1979).

[20] V. E. Dmitrienko and V. A. Belyakov, Sov. Phys. JETP **51**, 787 (1980).

[21] P. Martinot-Lagarde, Mol. Cryst. Liq. Cryst. **66**, 381 (1981).

[22] J. E. Maclennan, N. A. Clark, and M. Handschy, in *Solitons in Liquid Crystals*, edited by L. Lam and J. Prost (Springer-Verlag, New York, 1992), pp. 151–190.

[23] J. Fünfschilling and M. Schadt, Jpn. J. Appl. Phys., Part 1 **35**, 5765 (1996).

[24] M. Brunet and P. Martinot-Lagarde, J. Phys. II **6**, 1687 (1996).

[25] P. Mach, R. Pindak, A. M. Levelut, P. Barois, H. T. Nguyen, C. C. Huang, and L. Furenlid, Phys. Rev. Lett. **81**, 1015 (1998).

[26] P. Mach, R. Pindak, A. M. Levelut, P. Barois, H. T. Nguyen, H. Baltes, M. Hird, K. Toyne, A. Seed, J. W. Goodby, C. C. Huang, and L. Furenlidy, Phys. Rev. E **60**, 6793 (1999).

[27] M. Skarabot, M. Cepic, B. Zeks, R. Blinc, G. Heppke, A. V. Kityk, and I. Musevic, Phys. Rev. E **58**, 575 (1998).

[28] V. Laux, N. Isaert, V. Faye, and H. T. Nguyen, Liq. Cryst. **27**, 81 (2000).

[29] D. Schlauf, C. Bahr, and H. T. Nguyen, Phys. Rev. E **60**, 6816 (1999).

[30] P. M. Johnson, S. Pankratz, P. Mach, H. T. Nguyen, and C. C. Huang, Phys. Rev. Lett. **83**, 4073 (1999).

[31] D. A. Olson, S. Pankratz, P. M. Johnson, A. Cady, H. T. Nguyen, and C. C. Huang, Phys. Rev. E **63**, 061711 (2001).

[32] T. Sako, Y. Kimura, R. Hayakawa, N. Okabe, and Y. Suzuki, Mol. Cryst. Liq. Cryst. Sci. Technol., Sect. A **263**, 81 (1995).

[33] A. Cady, X. F. Han, D. A. Olson, H. Orihara, and C. C. Huang, Phys. Rev. Lett. **91**, 125502 (2003).

[34] A. Cady, D. A. Olson, X. F. Han, H. T. Nguyen, and C. C. Huang, Phys. Rev. E **65**, 030701(R) (2002).

[35] C. C. Huang, Z. Q. Liu, A. Cady, R. Pindak, W. Caliebe, P. Barois, H. T. Nguyen, K. Ema, K. Takekoshi, and H. Yao, Liq. Cryst. **31**, 127 (2004).

[36] T. Isozaki, T. Fujikawa, H. Takezoe, A. Fukuda, T. Hagiwara, Y. Suzuki, and I. Kawamura, Phys. Rev. B **48**, 13439 (1993).

[37] T. Isozaki, K. Hiraoka, Y. Takanishi, H. Takezoe, A. Fukuda, Y. Suzuki, and I. Kawamura, Liq. Cryst. **12**, 59 (1992).

[38] Y. Takanishi, K. Hiraoka, V. K. Agrawal, H. Takezoe, A. Fukuda, and M. Matsushita, Jpn. J. Appl. Phys., Part 1 **30**, 2023 (1991).

[39] M. Cepic, G. Heppke, J.-M. Hollidt, D. Lötzsch, D. Moro, and B. Zeks, Mol. Cryst. Liq. Cryst. Sci. Technol., Sect. A **263**, 207 (1995).

[40] K. Yamada, Y. Takanishi, K. Ishikawa, H. Takezoe, A. Fukuda, and M. A. Osipov, Phys. Rev. E **56**, R43 (1997).

[41] M. Glogarova, H. Sverenyak, A. Fukuda, and H. Takezoe, Liq. Cryst. **14**, 463 (1993).

[42] V. Laux, N. Isaert, G. Joly, and H. T. Nguyen, Liq. Cryst. **26**, 361 (1999).

[43] V. P. Panov, N. M. Shtykov, A. Fukuda, J. K. Vij, Y. Suzuki, R. A. Lewis, M. Hird, and J. W. Goodby, Phys. Rev. E **69**, 060701(R) (2004).

[44] V. Bourny and H. Orihara, Phys. Rev. E **63**, 021703 (2001).

[45] D. Konovalov and S. Sprunt, Phys. Rev. E **58**, 6869 (1998).

[46] K. Hiraoka, Y. Takanishi, K. Skarp, H. Takezoe, and A. Fukuda, Jpn. J. Appl. Phys., Part 2 **30**, L1819 (1991).

[47] S. Tatemori, H. Uehara, J. Hatano, H. Saito, S. Saito, and E. Okabe, Jpn. J. Appl. Phys., Part 1 **38**, 5657 (1999).

[48] J. P. F. Lagerwall, P. Rudquist, S. T. Lagerwall, and B. Stebler, Ferroelectrics **277**, 553 (2002).

[49] It is easy to show that for small θ the director reorientation, δ, in a phase where the only type of director modulation is the

helix, is equal to θ, i.e., we always have $\delta \approx \theta$ for very small tilt in Sm-C_α^* and Sm-C^*.

[50] The accuracy is rather low since the small P_s value close to Sm-A^* leads to large sensitivity to the integration limits as well as to the correctness in base line subtraction.

[51] S. Zhang, B. Wen, S. S. Keast, M. E. Neubert, P. L. Taylor, and C. Rosenblatt, Phys. Rev. Lett. **84**, 4140 (2000).

[52] B. Wen, S. Zhang, S. S. Keast, M. E. Neubert, P. L. Taylor, and C. Rosenblatt, Phys. Rev. E **62**, 8152 (2000).

[53] P. Rudquist, J. P. F. Lagerwall, J. G. Meier, K. D'havé, and S. T. Lagerwall, Phys. Rev. E **66**, 061708 (2002).

[54] A. Boulbitch and P. Tolédano, Eur. Phys. J. B **6**, 355 (1998).

[55] K. Hiraoka, Y. Takanishi, H. Takezoe, A. Fukuda, T. Isozaki, Y. Suzuki, and I. Kawamura, Jpn. J. Appl. Phys., Part 1 **31**, 3394 (1992).

[56] J. P. F. Lagerwall, D. D. Parghi, D. Krüerke, F. Gouda, and P. Jägemalm, Liq. Cryst. **29**, 163 (2002).

[57] V. A. Lapanik, A. A. Muravski, S. Y. Yakovenko, W. Drzewinski, K. Czuprynski, and R. Dabrowski, Ferroelectrics **244**, 429 (2000).

[58] H. Moritake, N. Shigeno, M. Ozaki, and K. Yoshino, Liq. Cryst. **14**, 1283 (1993).

[59] E. Gorecka, D. Pociecha, M. Cepic, B. Zeks, and R. Dabrowski, Phys. Rev. E **65**, 061703 (2002).

[60] J. P. F. Lagerwall, P. Rudquist, S. T. Lagerwall, and F. Giesselmann, Liq. Cryst. **30**, 399 (2003).